ChemComm

Accepted Manuscript

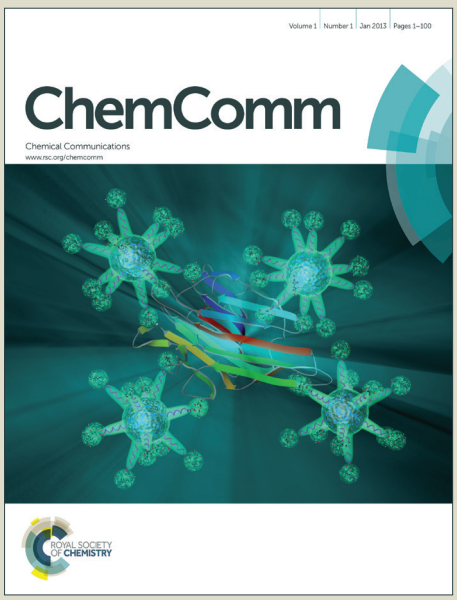

ROYAL SOCIETY OF CHEMISTRY

www.rsc.org/chemcomm

Cite this: DOI: 10.1039/c0xx00000x

www.rsc.org/xxxxxx

COMMUNICATION

Three Dimensional Nano-assemblies of Noble Metal Nanoparticles-Infinite Coordination Polymers as A Specific Oxidase Mimetic for Degradation of Methylene Blue without Adding Cosubstrate

Lihua Wang,Yi Zeng, Aiguo Shen,* Xiaodong Zhou, and Jiming Hu*

Received (in XXX, XXX) XthXXXXXXXXX 20XX, Accepted Xth XXXXXXXXX 20XX
DOI: 10.1039/b000000x

Novel three-dimensional (3D) nano-assemblies of noble metal nanoparticles (NPs)-infinite coordination polymers (ICPs) are conveniently fabricated through the infiltration of $HAuCl_4$ into hollow Au@Ag@ICPs core-shell nanostructures and its replacement reaction with Au@Ag NPs. The present 3D nano-assemblies exhibit highly efficient and specific intrinsic oxidase-like activity even without adding any cosubstrate.

Due to high substrate specificity and catalytic activity under mild conditions, natural enzymes have been attracting great interest in pharmaceutical processes, biosensing, agrochemical production, and food industry applications.[1-2] However, they still bear some intrinsic drawbacks such as denaturation resulted poor stability, low sensitivity of catalytic activity owing to environmental conditions and difficulties of fabricating.[3-4] Researchers therefore endeavoured to develop the artificial enzyme mimetic as a viable alternative to natural enzyme. Since the first exciting discovery of ferromagnetic nanoparticles (NPs),[5] more and more well-known single-component nanomaterials with intrinsic peroxidase- or oxidase-like activity emerged in succession, such as noble metal NPs,[6-8] metal oxide,[9-11] carbon-based nanomaterials[12-14] and so on.

In comparison with natural enzymes, these nanoparticulate alternatives exhibit several advantages including low-price, easy preparation, high stability against denaturing, and tunability in catalytic activities. The most remarkable of these is gold NPs.[15] For example, positively-charged gold NPs[16] (with diameter about 34 nm) possess intrinsic peroxidase-like activity and can be used to detect H_2O_2 and glucose with colorimetric method; "naked" gold NPs[17] are found to be able to catalytically oxidize glucose with the cosubstrate oxygen (O_2) similar to glucose oxidase. Besides, Au NPs also exhibited intrinsic superoxide dismutase-like and catalase-mimetic activity[18] at physiological pH or under alkaline conditions, respectively, *etc*. Even though, most of the single-component artificial enzyme mimetics possess relatively low catalytic activity and gold NPs are no exception.[16] Furthermore, it is widely acceptable that two key factors including particle size and its dispersion determine the catalytic performance of gold NPs.[19] To enhance the dispersion of the gold NPs in smaller sizes and meantime maintain their catalytic activity, they were often impregnated into or deposited onto low-cost and electronically transmitted supporting materials (such as inorganic substances and organic polymers).[4, 19] Therefore, a new generation of gold-bearing composite catalysts[20-22] have recently been particularly impressive because they benefit from the synergistic effect and/or the electronic effect of multiplex components besides highly dispersed smaller-sized gold NPs.[23] For example, Zhang *et al.* demonstrated that nano-hybrids[24] of Au NPs and single-walled carbon nanotubes (SWCNTs) possessed remarkably enhanced peroxidase-like activity compared to the sole positively-charged Au NPs or SCWNTs; Liu *et al.* found the Au NPs-graphene sheets hybrids[23] exhibit a synergetic effect in mimicking peroxidase.

In this work, a simple approach is suggested to fabricate novel noble metal NPs-infinite coordination polymers (ICPs) three-dimensional (3D) nano-assemblies based on our previous research.[25] The obtained 3D nano-assemblies exhibit highly efficient and specific intrinsic oxidase-like activity for degradation of methylene blue (MB) even without adding any cosubstrate, *e.g.*, H_2O_2. In this synthesis, the as-prepared Au@Ag-ICPs hollow core-shell nanostructures (Au@Ag@void @ICPs) are proposed as active precursors and 3D host frameworks for the infiltration of $HAuCl_4$ and its subsequent *in situ* replacement reaction with silver shell of Au@Ag core, because the DMcT-based ICPs shell is highly porous and beneficial for the penetration of water-soluble small molecules. Besides, DMcT is known to be one of the most promising organosulfur compounds as a cathode active material.[26] So, the DMcT-based ICPs should be beneficial for the oxidation of 3,3′,5,5′-Tetramethylbenzidine (TMB) and MB, which is an electron transfer process.

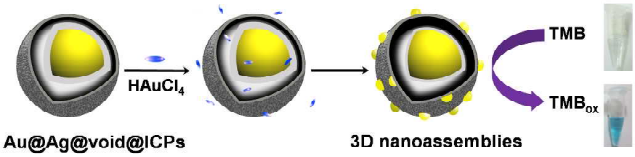

Fig. 1 Illustration of the procedure used to prepare 3D nano-assemblies with specific oxidase-like activity.

The 3D nano-assemblies were synthesized by simply adding some volume of $HAuCl_4$ into the stirring solution of Au@Ag@void@ICPs (**Fig. 1**). In this process, the solution's colour changes from orange to purple. Meanwhile, the silver peak belonging to Au@Ag@void@ICPs disappeared and only a wider peak at *ca.* 550 nm appeared (**Fig. S1, ESI**). It should be noted that the latter had obvious red shift in comparison with that of 30 nm Au NPs at the very beginning and meanwhile no obvious aggregation happened in this process, indicating a new nanostructure had been produced. **Fig. 2A** shows a typical transmission electron microscopy (TEM) image of the final

product. It can be clearly seen that some small Au NPs with

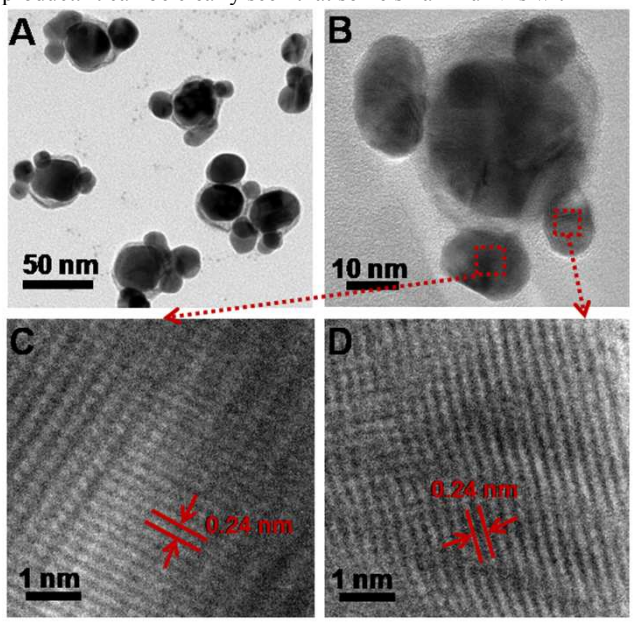

Fig. 2 (A-B) TEM and (C-D) HRTEM images of 3D nano-assemblies.

diameters of approximately 14.6 nm (**Fig. S2, ESI**) are asymmetrically interspersed onto the shell of Au@Ag@void@ICPs (**Fig. 2B**) and a new highly dispersed 3D nano-assembly is prepared without additional chemical or bio-molecular stabilizers. **Fig. 2C and 2D** further show the HRTEM lattice image of the Au NPs. The lattice spacing of 0.24 nm, marked in these two pictures, is consistent with that of Au (111) planes.[27] Besides, X-ray photoelectron spectroscopy (XPS, **Fig. S3, ESI**) analysis indicates that such nano-assemblies contain elements of Au, Ag, C, S, N, O and Cl. Among them, the elemental concentration of Ag is larger than that of Cl (**Table S1, ESI**). Factually, in our experiment, white solid AgCl precipitates were found to settle at the bottom of the container after the products placed for a period of time. Thus, the Cl element here is ascribed to AgCl and C, S, N, and the extra Ag confirmed the existence of Ag-DMcT ICPs. Additionally, the O 1s peak at 532.3 eV in the XPS spectrum shown in **Fig. S3** indicated that there was chemisorbed oxygen on the surface of the 3D nano-assemblies.[28-29]

Given that galvanic replacement reaction between Au@Ag NPs and $HAuCl_4$ is the key point in our synthesis, the influences of the composition of Au@Ag NPs and the amount of $HAuCl_4$ on the products' nanostructure were further investigated. From **Figure S4**, we can see that the number of small Au NPs in the nano-assemblies gradually increases when the volume of $AgNO_3$ increases from 50 to 300 μL. Meanwhile, the products in these cases are highly dispersed. However, the products aggregate seriously when the volume of $AgNO_3$ increases to 500 μL, although the number of small Au NPs continues to increase. On the other hand, we also explored the influences of the volume of $HAuCl_4$ (**Fig. S5, ESI**). It is found that when the volume of $HAuCl_4$ is relatively small (5 μL), there are many small ellipsoidal Au NPs in 3D nano-assemblies with diameters less than 10 nm but they are easy to string together to form dendritic structures. When the volume of $HAuCl_4$ increases to 10 μL, the small Au NPs progressively grow up and are close to quasi-spheres. In this case, well-defined and mono-dispersed 3D nano-assemblies can be fabricated. Yet, when the volume of $HAuCl_4$ continues to increase (20 μL), the small Au NPs further grow up and reduces the distances of 3D nano-assemblies, which leads to

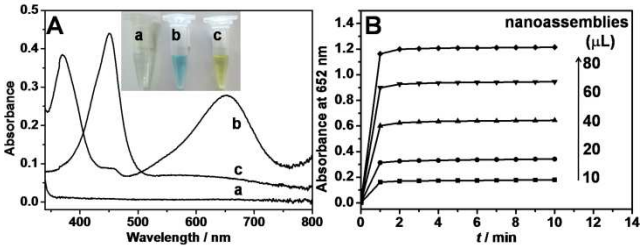

Fig. 3 (A) UV-*vis* spectra of the reaction solution containing TMB (a) in the absence of 3D nano-assemblies, (b) in the presence of 3D nano-assemblies, and (c) after quenched by H_2SO_4. Inset: photographs of different solutions corresponding to parts a-c. (B) Time-dependent absorbance changes at 652 nm in the presence of different volume of 3D nano-assemblies in BR buffer (pH 4.0) at room temperature.

the NPs' aggregation. Herein, it can be concluded that the number and size of small Au NPs in 3D nano-assemblies can be well modulated by the composition of Au@Ag NPs and the amount of $HAuCl_4$, respectively.

TMB, one of the most common HRP substrates in various bioassays, was used to investigate the oxidase-like activity of 3D nano-assemblies. As can be seen from **Fig. 3A**, 3D nano-assemblies can catalyze the fast oxidation of TMB within minutes without the presence of H_2O_2 to produce a blue colour with maximum absorbance at 652 and 370 nm. In contrast, no obvious reaction occurred in the absence of 3D nano-assemblies, suggesting the oxidase-like activity of the hybrids. Besides, we also attempted to perform an Au NP synthesis using only the ICP. It is found that obvious Au NPs can be hardly discerned in the final products (**Fig. S6, ESI**), which correspondingly results in poor catalysis of TMB (**Fig. S7, ESI**). These results indicate that Au@Ag NPs are an ideal template for the formation of dispersed ICPs and small-sized gold NPs under a mild condition. Like enzymatic peroxidase activity, such as observed for the commonly used enzyme HRP, this catalytic reaction could even be quenched by H_2SO_4.[13] The blue product was further oxidized to a yellow diimine with a maximum absorption wavelength of 450 nm. Besides, we investigated the effect of H_2O_2 on TMB oxidation (**Fig. S8, ESI**). It is found that the reaction did not get much faster with the involvement of H_2O_2—different from the properties of peroxidise-like enzymes, indicating the 3D nano-assemblies only possess specific oxidase-like activity. Moreover, a time-dependent absorbance change against concentration of 3D nano-assemblies was also observed (**Fig. 3B**). With the increasing of the volume of 3D nano-assemblies, the absorbance change was greatly improved. On the other hand, we compared the oxidation activity of 3D nano-assemblies at different pH values. From **Figure S9**, it can be seen as the pH value of the buffered solution increases from pH 4.0 to 7.0, the ability of 3D nano-assemblies to catalyze the TMB oxidation decreases. Meanwhile, at pH 8.0, no significant oxidation of TMB was observed, even upon overnight incubation (**Fig. S10**). These results suggest that the 3D nano-assemblies behaves as an oxidation catalyst in a pH-dependent manner and performs optimally at acidic pH values, which is similar to many other peroxidase-like or oxidase-like enzymes.[10, 14, 30]

As an oxidase mimic, the 3D nano-assemblies catalyze an oxidation-reduction reaction involving O_2 as the electron acceptor. It is reported that there are two kind of O_2, namely, dissolved oxygen and adsorbed oxygen in the reaction system of TMB-O_2-nanomaterials,[29] due to the high specific surface area of nanomaterials. In order to determine whether the dissolved O_2

played a role in the TMB-O_2-3D nano-assemblies system, two

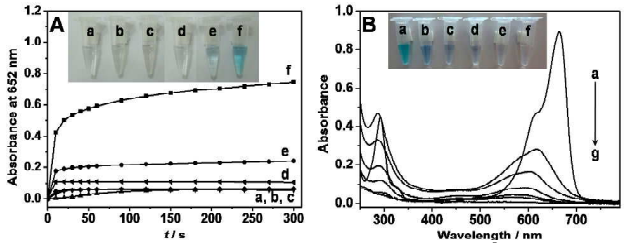

Fig. 4 (A) The absorbance evolution at 652 nm over time by different catalysts: (a) 30 nm Au NPs, (b) Au@Ag NPs, (c) Au@Ag@void@ICPs NPs, (d) Ag-DMcT ICPs, (e) Au@Ag NPs + $HAuCl_4$, and (f) 3D nano-assemblies. The inset shows the colour change of different samples. (B) Time-dependent UV-*vis* spectra and photographs of MB solution catalyzed by 3D nano-assemblies: (a) 0 min, (b) 1 min, (c) 3 min, (d) 6 min, (e) 10 min, (f) 20 min, and (g) 40 min.

sets of experiments were conducted: the first one was carried out in the presence of O_2; the other was performed under high-purity nitrogen (N_2) and the solution was degassed before the reaction. It is found that the reaction rate of TMB oxidation hardly changed after saturation with N_2 (**Fig. S11**). This indicated that the dissolved O_2 had no effect on the reaction, which was different from the behaviour of some NPs-based oxidase mimics reported.[31-32] Hence, it can be inferred that the adsorbed O_2 on the surface of 3D nano-assemblies oxidized TMB in this system. Besides, we investigated the electro-catalytic behaviour of a 3D nano-assemblies modified glassy carbon electrode (GCE) toward the electrochemical oxidation of TMB using cyclic voltammetry (CV). The CVs of TMB at a bare GCE and the 3D nano-assemblies-modified GCE are shown in **Fig. S12**. It is found that the redox peak current of TMB increased obviously under the 3D nano-assemblies-modified GCE, which is consistent with some mimetic enzyme related references.[29-30] To explore the reasons for the highly catalytic activity of 3D nano-assemblies, a series of control experiments were conducted (**Fig. 4A**). It can be seen that in our system, 30 nm Au NPs, Au@Ag NPs, Au@Ag@void@ICPs, and pure Ag-DMcT ICPs all hardly have catalytic activity toward the oxidation of TMB. And, when some volume of $HAuCl_4$ was introduced into the Au@Ag NPs solution to produce small gold NPs, the products weakly catalyze the oxidation of TMB and a light blue solution can be obtained. However, when the 3D nano-assemblies used instead, obvious catalysis appeared. The above results indicate that the highly catalytic activity of 3D nano-assemblies is due to the synergistic effect between small Au NPs and DMcT-Ag ICPs rather than small Au NPs only. In this process, much more TMB is absorbed on the surface of the 3D nano-assemblies, due to the highly porosity of ICPs, which results in an increase of the local concentration of reactants in the nano-assemblies. Besides, it is well known that DMcT is one of the most promising organosulfur compounds as a cathode active material and the conductivity of poly [di (2,5-dimercapto-1,3,4-thiadiazole)]-metal complexes will increase as temperature goes up.[33] Combined with the mechanism described as above, the DMcT-Ag ICPs here may have the ability to accelerate the electron transfer from 3D nano-assemblies to absorbed O_2, thus increasing the reaction rate of TMB oxidation.

Next, the oxidase-like catalytic property of the 3D nano-assemblies was further investigated at various pH values using steady-state kinetics and typical Michaelis-Menten curves were obtained (**Fig. S13**). Results show that as the solution's pH value increases, larger values for the Michaelis constant (K_m) and lower values for the reaction rate (V_{max}) are obtained (**Table S2**). Specifically, the K_m of 3D nano-assemblies with TMB as the substrate is as low as 4.31 μM at pH 4.0, which is about one or two hundred times lower than HRP, Fe_3O_4 MNPs (magnetic nanoparticles) and CeO_2 (**Table S3**), suggesting that the 3D nano-assemblies have a higher affinity for TMB than others.

Organic dyes, as common pollutants from wastewater, were one of the most detected targets in water analysis. Currently, the common approaches to degrade dyes (such as MB) are usually based on nanocatalysts with the aid of $NaBH_4$,[19] or H_2O_2,[34] or UV irradiation[35] and so on. Although much progress has been made, some drawbacks need to be improved for the above methods: $NaBH_4$ is easy to absorb water from the air and then deteriorates; H_2O_2 decomposes upon prolonged storage and losses its ability; UV irradiation needs harsh experimental conditions like light intensity, reactor geometry, *etc*. As a result, more stable and convenient methods are needed for the degradation of dyes. Based on the excellent catalytic activity of 3D nano-assemblies to the oxidation of TMB, they were further tested for MB degradation without the presence of H_2O_2. MB aqueous solution has maximum UV-*vis* absorption (A_{max}) at 663 and 614 nm. The catalytic degradation process of MB can be monitored by the decrease of A_{max} intensity. **Fig. 4B** shows a typical evolution process of the UV-*vis* spectra of MB during the catalytic degradation with the 3D nano-assemblies. It can be observed that a sharp decrease in absorption with an obvious concomitant wavelength shift of the band to shorter wavelengths happened within 40 min, indicating that the oxidative degradation catalyzed by the 3D nano-assemblies is superior to the reported photocatalytic degradation without adding any cosubstrate.[35] Meantime, in this process, the solution's colour changes from sky blue to light blue, and then light purple, and finally almost colourless. Noted that these phenomena are very similar to the report by Zhang *et al.*,[35] in which they found that *N*-demethylation of MB happened before its complete degradation. In addition, some control experiments were also conducted. It is found that only a small amount of MB molecules were degraded even after 40 min in the presence of pure Au NPs, Au@Ag NPs, Au@Ag@void@ICPs NPs, or in the absence of any catalyst (**Fig. S14**). Meanwhile, we also did the degradation of MB with 3D nano-assemblies at room temperature (**Fig. S15**). It is found that a small portion of MB molecules cannot be degraded even after 40 min, which indicated that the temperature (80°C) is very significant for the degradation of MB. On the other hand, we compared the oxidase-like activity of the 3D nano-assemblies at room temperature and 80°C (**Fig. S16**). It is found that no obvious decrease happened, which indicated that the 3D nano-assemblies show excellent thermal stability. The above results indicate that the 3D nano-assemblies also delivered highly catalytic activity for the catalytic oxidation of MB even in the absence of additional cosubstrate.

Conclusions

In summary, we present a very simple and controllable method to prepare novel noble metal nanoparticles (NPs)-infinite coordination polymers (ICPs) 3D nano-assemblies. These 3D nano-assemblies are found to possess specific oxidase-like activity and could catalyze the oxidation of TMB to produce the typical colour reaction by the O_2 absorbed on the surface of the 3D nano-assemblies rather than H_2O_2. In addition, due to the

synergistic effect between DMcT-Ag ICPs and highly dispersed small gold NPs, the obtained 3D nano-assemblies have excellent catalytic performance with regard to the degradation of MB.

Notes and references

Key Laboratory of Analytical Chemistry for Biology and Medicine, Ministry of Education, College of Chemistry and Molecular Sciences, Wuhan University, 430072 Wuhan (P. R. China). Fax: 0086-27-68752136; Tel: 0086-27-68752439; E-mail: agshen@whu.edu.cn, jmhu@whu.edu.cn.

† Electronic Supplementary Information (ESI) available: Experimental details, characterization data of UV-*vis*, XPS, TEM and SEM, evaluation of the oxidase-like activity, studies on possible mechanism of the catalytic oxidation of TMB by cyclic voltammetry and control experiments on the degradation of MB. See DOI: 10.1039/b000000x/

‡ This work was financially supported by National Natural Science Foundation of China (No. 21175101), National Major Scientific Instruments and Device Development Project (No. 2012YQ16000701), Foundation of China Geological Survey (No. 12120113015200), and the Fundamental Research Funds for the Central Universities (No. 2042014kf0260).

1 Hult, K.; Berglund, P. *Curr. Opin. Biotechnol.* **2003**, *14*, 395-400.
2 Barber, J. *Chem. Soc. Rev.* **2009**, *38*, 185-196.
3 Wagner, J.; Lerner, R. A.; Barbas, C. F. *Science* **1995**, *270*, 1797-1800.
4 Zhang, L. N.; Deng, H. H.; Lin, F. L.; Xu, X. W.; Weng, S. H.; Liu, A. L.; Lin, X. H.; Xia, X. H.; Chen, W. *Anal. Chem.* **2014**, *86*, 2711-2718.
5 Gao, L. Z.; Zhuang, J.; Nie, L.; Zhang, J. B.; Zhang, Y.; Gu, N.; Wang, T. H.; Feng, J.; Yang, D. L.; Perrett, S.; Yan, X. Y. *Nat. Nanotechnol.* **2007**, *2*, 577-583.
6 Wu, Y. S.; Huang, F. F.; Lin, Y. W. *ACS Appl. Mater. Interfaces* **2013**, *5*, 1503-1509.
7 Lien, C. W.; Huang, C. C.; Chang, H. T. *Chem. Commun.* **2012**, *48*, 7952-7954.
8 Ni, P. J.; Dai, H. C.; Wang, Y. L.; Sun, Y. J.; Shi, Y.; Hu, J. T.; Li, Z. *Biosens. Bioelectron.* **2014**, *60*, 286-291.
9 Zhang, L. L.; Han, L.; Hu, P.; Wang, L.; Dong, S. J. *Chem. Commun.* **2013**, *49*, 10480-10482.
10 Asati, A.; Santra, S.; Kaittanis, C.; Nath, S.; Perez, J. M. *Angew. Chem. Int. Ed.* **2009**, *48*, 2308-2312.
11 André, R.; Natálio, F.; Humanes, M.; Leppin, J.; Heinze, K.; Wever, R.; Schröder, H. C.; Müller, W. E. G.; Tremel, W. *Adv. Funct. Mater.* **2011**, *21*, 501-509.
12 Li, R. M.; Zhen, M. M.; Guan, M. R.; Chen, D. Q.; Zhang, G. Q.; Ge, J. C.; Gong, P.; Wang, C. R.; Shu, C. Y. *Biosens. Bioelectron.* **2013**, *47*, 502-507.
13 Song, Y. J.; Qu, K. G.; Zhao, C.; Ren, J. S.; Qu, X. G. *Adv. Mater.* **2010**, *22*, 2206-2210.
14 Cui, R. J.; Han, Z. D.; Zhu, J. J. *Chem. Eur. J.* **2011**, *17*, 9377-9384.
15 Lin, Y. H.; Ren, J. S.; Qu, X. G. *Adv. Mater.* **2014**, *26*, 4200-4217.
16 Jv, Y.; Li, B. X.; Cao, R. *Chem. Commun.* **2010**, *46*, 8017-8019.
17 Comotti, M.; Pina, C. D.; Matarrese, R.; Rossi, M. *Angew. Chem. Int. Ed.* **2004**, *43*, 5812-5815.
18 He, W. W.; Zhou, Y. T.; Wamer, W. G.; Hu, X. N.; Wu, X. C.; Zheng, Z.; Boudreaud, M. D.; Yin, J. J. *Biomaterials* **2013**, *34*, 765-773.
19 Gan, Z. B.; Zhao, A. W.; Zhang, M. F.; Tao, W. Y.; Guo, H. Y.; Gao, Q.; Mao, R. R.; Liu, E. H. *Dalton Trans.* **2013**, *42*, 8597-8605.
20 Tao, Y.; Lin, Y. H.; Huang, Z. Z.; Ren, J. S.; Qu, X. G. *Adv. Mater.* **2013**, *25*, 2594-2599.
21 Lee, J. W.; Jeon, H. J.; Shin, H. J.; Kang, J. K. *Chem. Commun.* **2012**, *48*, 422-424.
22 Santos, R. M.; Rodrigues, M. S.; Laranjinha, J.; Barbosa, R. M. *Biosens. Bioelectron.* **2013**, *44*, 152-159.
23 Liu, M.; Zhao, H. M.; Chen, S.; Yu, H. T.; Quan, X. *ACS Nano* **2012**, *6*, 3142-3151.
24 Zhang, Y. F.; Xu, C. L.; Li, B. X.; Li, Y. B. *Biosens. Bioelectron.* **2013**, *43*, 205-210.
25 Wang, L. H.; Shen, A. G.; Li, X. C.; Zeng, Y.; Zhou, X. D.; Richards, R. M.; Hu, J. M. *RSC Adv.* **2014**, *4*, 34294-34302.
26 Kiya, Y.; Hutchison, G. R.; Henderson, J. C.; Sarukawa, T.; Hatozaki, O.; Oyama, N.; Abruña, H. D. *Langmuir* **2006**, *22*, 10554-10563.
27 Xie, W.; Su, L.; Donfack, P.; Shen, A. G.; Zhou, X. D.; Sackmann, M.; Materny, A.; Hu, J. M. *Chem. Commun.* **2009**, 5263-5265.
28 Wu, Z. B.; Jin, R. B.; Liu, Y.; Wang, H. Q. *Catal. Commun.* **2008**, *9*, 2217-2220.
29 Qin, W. J.; Su, L.; Yang, C.; Ma, Y. H.; Zhang, H. J.; Chen, X. G. *J. Agric. Food Chem.* **2014**, *62*, 5827-5834.
30 Chen, Q.; Liu, M. L.; Zhao, J. N.; Peng, X.; Chen, X. J.; Mi, N. X.; Yin, B. D.; Li, H. T.; Zhang, Y. Y.; Yao, S. Z. *Chem. Commun.* **2014**, *50*, 6771-6774.
31 He, W. W.; Liu, Y.; Yuan, J. S.; Yin, J. J.; Wu, X. C.; Hu, X. N.; Zhang, K.; Liu, J. B.; Chen, C. Y.; Ji, Y. L.; Guo, Y. T. *Biomaterials* **2011**, *32*, 1139-1147.
32 Zhao, J. K.; Xie, Y. F.; Yuan, W. J.; Li, D. X.; Liu, S. F.; Zheng, B.; Hou, W. G. *J. Mater. Chem. B* **2013**, *1*, 1263-1269.
33 Shekeil, A. G. E.; Maydama, H. M. A.; Shujáa, O. M. A. *J. Appl. Polym. Sci.* **2007**, *106*, 2427-2435.
34 Kundu, J.; Pradhan, D. *ACS Appl. Mater. Interfaces* **2014**, *6*, 1823-1834.
35 Zhang, T.; Oyama, T.; Aoshima, A.; Hidaka, H.; Zhao, J. C.; Serpone, N. *J. Photochem. Photobiol. A* **2001**, *140*, 163-172.